RADIOMETRIC PROCESSING OF ADS IMAGERY: MOSAICKING OF LARGE IMAGE BLOCKS

Stephan Gehrke
North West Geomatics
Suite 212, 5438 – 11th Street NE
Calgary, Alberta, T2E 7E9, Canada
stephan.gehrke@nwgeo.com

ABSTRACT

Orthoimage mosaics presume radiometric adaptation of the individual images, which is referred to as relative radiometric normalization (RRN). This paper presents an in-house developed RRN approach that aims for optimal adaptation of large blocks of Leica ADS line-scanner imagery for subsequent mosaicking. It assumes orthorectified and radiometrically preprocessed input image data – with camera calibration, atmospheric and BRDF corrections applied as described in a companion paper – but still allows for the adaptation of bigger radiometric differences. The RRN model incorporates the adaptation of brightness and contrast, both varying throughout each image according to location-dependent polynomials. Correction parameters are derived from corresponding, invariant points within image overlaps; water areas are generally excluded to ensure smooth transitions over land. The computation is carried out as a block-wide least squares adjustment, combining both local adaptation of overlapping areas and global normalization of the mosaic. This RRN processing is used in North West Geomatics' production since 2009 and has been applied to numerous ADS blocks. An example from TNRIS (Texas Natural Resources Information System) data is presented.

INTRODUCTION

In order to provide uniform geometry and homogenous radiometry throughout large areas, individual orthoimages have to be mosaicked. The proceeding adaptation of radiometric differences between these images is commonly referred to as relative radiometric normalization (RRN). There is a broad variety of research papers that discuss RRN for different purposes, including mosaicking but mainly concentrating on the adaptation of two or more images for visual comparison, change detection, or classification (see overviews in: Yang and Lo, 2000; Over et al., 2003; Hong, 2007). Accordingly, RRN is implemented in research-oriented and also commercial software products. However, professional mosaicking packages are often designed for frame imagery and handle Leica ADS and other line-scanner data by dividing the long flight lines (takes) of up to 1,000,000 pixels into sub-chunks that are treated independently. This leads to the – unnecessary – introduction of seam lines along with radiometric adaptations within single line-scanner images.

The purpose of the presented in-house development is the automatic radiometric adjustment of Leica ADS blocks – a precondition for mosaicking. It is based on image data that are pre-corrected as described in a companion paper, "Radiometric Processing of ADS Imagery: Using Atmospheric and BRDF Corrections in Production" (Downey et al., 2010). Nevertheless, the RRN is required to still allow for the adaptation of major radiometric differences, since large blocks – in some cases more than 100 ADS flight lines – are flown at different times of day and often with different cameras or even in different season, e.g. in case of partial re-flights. Such radiometric complexity cannot be described to the full extent by atmospheric and BRDF models and remaining differences need to be adjusted by RRN. For the purpose of seamless mosaicking, neighboring image takes have to be adapted in their overlapping areas to eventually place seam lines and allow for proper blending. The adjustment includes reference images of already existing, neighboring mosaics to enable a seamless transition across blocks as well. In addition to such local adaptation, a global homogenization throughout the mosaic is desired and for large blocks usually required. This could mean either to retain the (average) radiometry of the input data or to alter the mosaic to a reference such as a neighboring block.

Geometrically, it is a pre-requisite that all input images are orthorectified to the same coordinate system, which guarantees that features such as radiometric tie points can be obtained at identical ground coordinates. Nevertheless, radiometric mismatches might occur due to differing shadows, specular reflectance in water bodies or, occasionally, land cover and vegetation changes. Respective points must be eliminated to base RRN on invariant tie points only.

The remainder of this paper begins with a survey of existing RRN approaches. Based on that, a suitable model for the normalization of ADS line-scanner images is presented, which – considering the requirements on the mosaic's radiometry as well as border conditions – needs to be carried out as a global, integrated adjustment. The evaluation of radiometric tie points is discussed in detail. Finally, normalization results are presented for a block that is typical for the North West Geomatics production work-flow.

OVERVIEW ON RRN APPROACHES

RRN has to consider various aspects, mainly the functional model for histogram adaptation, the spatial validity of this model, and the radiometric features or tie points used for parameter computation. The normalization of multi-band imagery – in case of the ADS: red, green, blue, and near infrared (NIR) – is discussed in that context.

Histogram Adaptation

The adaptation of histograms of individual image bands can be based on bias (brightness), linear correction (brightness and contrast), or more complex modifications. The simplest way accounts for the bias between individual histograms. Homer et al. (1997) use this approach to adjust satellite images, at the same time aiming for maintaining radiometric characteristics for classification. A much better homogenization of a mosaic can be achieved by introducing an additional scaling parameter, which leads to a linear function that comprises brightness, b, and contrast, c. Then original image DNs are corrected by RRN as follows:

$$DN_{RNN}(x, y) = b + c\ DN(x, y) \tag{1}$$

Based on this equation, either one image can be adapted to match another or the images can be altered towards a common target. Such linear normalization is mathematically simple and practically effective; it is by far the most widely used function. There exists a variety of approaches for the derivation of contrast and brightness from corresponding points, in particular:

- Least squares adjustment (LSA) or linear regression (Galiatsatos et al., 2007; Scheidt et al., 2008): The estimation of contrast and brightness corrections for adapting one image to a reference is based on the observation equation (1) above. The LSA will inherently provide accuracy information for the estimated parameters as well as further statistics.
- Standard deviation: This method is a widely used approximation of the LSA, based on the common definition of contrast as the standard deviation. The contrast correction is provided by the relation of the images' DN standard deviations; brightness follows from the difference of mean DNs (Afek and Brand, 1998; Jessop and Schickler, 2000; Nobrega and Quintanilha, 2004; Brown and Lowe, 2007). While this method will lead to the same coefficients as the LSA in the case of a truly linear connection between the histograms of both images, it does not minimize the squared sum of residuals in general.
- Min-max method: Histogram adaptation is based on minimum and maximum DNs in both images. Contrast is computed as the relation of differences of these DNs, brightness follows accordingly. This method needs to imply some meaningful threshold to identify significant minima and maxima in order to exclude extremely dark or bright outliers (cp. Janzen et al., 2006).
- Dark-bright method: Similar to min-max, parameter computation is based on average DNs of dark and bright pixel sets in both images. This method involves classification to derive these so-called radiometric control sets (Yang and Lo, 2000; Hong, 2007).

A more complex, non-linear histogram matching should allow for an even closer adaptation because it minimizes differences in histogram shapes rather than performing an overall (linear) adaptation. It is essentially based on look-up tables (Yang and Lo, 2000; Nielsen, 2004; Tsai and Huang, 2005).

Different RRN functions have been compared with regard to radiometric differences that remain after correction by Yuan and Elvridge (1996), Yang and Lo (2000), Over et al. (2003), Ding et al. (2005), Hong (2007), and Scheidt et al. (2008). Although in most of these tests the histogram adaptation approach is combined with a specific method for radiometric tie point extraction (see following section for the latter), the superior performance of the linear regression (LSA) has been found in almost all tests; non-linear models, although theoretically allowing for closer histogram matches, do not perform better in practical applications. The other above-listed methods tend to be more

sensitive to the data set and/or the tie point quality, with min-max generally ranked lowest. Regarding the preservation of image statistics, Yang and Lo (2000) found that the approaches that ensure the best fit tend to perform less successful in maintaining relative variability. However, the significant dynamic range reduction they found using a linear regression stands in contrast to Canty et al. (2004), who investigated a similar, orthogonal regression.

Considerations for Multi-Band Images

The above-described methods aim for the adaptation of corresponding DN pairs and, therefore, pertain to individual bands. In practice, RRN techniques are applied to all bands independently without regarding for any interconnections; see respective descriptions in Homer et al. (1997), Yang & Lo (2000), Over et al. (2003), Xandri et al. (2005), Galiatsatos et al. (2007), Hong (2007), El Hajj (2008), Falala et al. (2008), and Scheidt et al. (2008). Nobrega and Quintanilha (2004) point out that normalization needs to be independent for each band to achieve the best color balancing.

Nielsen (2004) analyses histograms in different color spaces, RGB and IHS, before and after performing separate RRNs on the RGB bands. He finds that this approach is suited to nicely match hues without specifically aiming for their adaptation by normalizing in IHS space. The color-space independency is not only important for RGB but especially for the NIR band as there is no conversion into perceptual units.

Spatial Resolution of RRN Parameters

The vast majority of RRN approaches – Jessop and Schickler (2000), Brown and Lowe (2007), El Hajj (2008), and the papers on normalization of satellite imagery listed in the references – assumes a set of spatially constant correction parameters within overlapping areas, mainly because it combines simplicity with the desired accuracy. For mosaicking, this assumption is often extended to entire images, with parameters derived from overlaps (Homer et al., 1997; Tsai and Huang, 2005; Scheidt et al., 2008). Some mosaicking approaches divide images into sub-blocks (Uyttendaele et al. 2001; Nobrega and Quintanilha, 2004), where individual sets of transformation parameters are retrieved. This might cause blocking artifacts, which need to be overcome by conditions, subsequent adjustment and/or blending. It also introduces artificial seam lines and, accordingly, blending within original images.

A more sophisticated method is to allow for spatially varying normalization parameters, i.e. to introduce a functional dependency on line and sample within each image (Afek and Brand, 1998; Falala et al., 2008). This spatial variation would address remaining errors and/or effects not modeled in camera calibration and atmospheric or BRDF corrections, which depend on illumination and viewing geometry and, therefore, have different impact on different parts of the image. Such an adaptive parameterization will be necessary for normalizing very long ADS images.

Radiometric Tie Points (Invariant Features)

Normalization parameters can be derived from all points within image overlaps. Some mosaicking approaches only consider areas around known seam lines (Afek and Brand, 1998; Tsai and Huang, 2005). In practice, most RRN methods involve classification or validation of radiometric tie points to find an invariant subset, such as:

- Manual masking of no-change areas (e.g.: Over et al., 2003).
- Classification: There exists a large number of different methods – see descriptions and comparisons in Yang and Lo (2000), Over et al. (2003) or Hong (2007): pseudo-invariant features (typically man-made objects), identified by a combination of red and NIR bands; dark (water) and bright (urban) radiometric control sets, derived from all color bands using Knauth-Thomas greenness-brightness scattergrams; no-change sets (stable water and stable land), which are obtained using multiple infrared bands or even all available bands (Jantzen et al., 2006). In addition to these validations and similar to Downey et al. (2010), water can be classified based on the NDVI and omitted to achieve the best RRN across land areas.
- Statistical methods: multivariate alteration detection, a generalized eigenvalue problem using linear combinations of DNs of all bands (Over et al., 2003; Canty et al., 2004); principal components analysis, based on variance-covariance matrices of DNs in overlapping images (Galiatsatos et al., 2007); pixel-based across-band correlation coefficients (Scheidt et al., 2008).

In terms of minimizing radiometric differences, the classification methods improve with increasing complexity (Yuan and Elvridge, 1996; Ding et al., 2005; Hong, 2007), although the best performance of no-change sets might be at least partly explained by its usual combination with the linear regression. Somewhat surprisingly, the regres-

sion delivers similar results with or without prior classification (Yang and Lo, 2000; Ding et al., 2005; Scheidt et al., 2008). Unfortunately, there is little evaluation on how classification compares to statistical methods but the tests of Over et al. (2003) indicate that the latter provide better tie point sets than classification-based approaches. Over et al. (2003) and Scheidt et al. (2008) found that the regression benefits from evaluating radiometric tie points with statistical methods such as the across-band correlation, which, in conclusion, makes this combination the desired RRN approach.

RRN FOR MOSAICKING LARGE ADS BLOCKS

Based on the fact that the linear regression provides the best fit, such a least squares adjustment approach is extended to the entire image block, involving all overlapping areas. Conditions on global mosaic radiometry as well as reference images can be integrated in such an adjustment.

Histogram Adaptation Model

The RRN approach for large ADS blocks is based on a linear model that adapts brightness and contrast. Despite its empirical character, it is a good proxy for camera calibration as well as for atmospheric and BRDF corrections if applied locally: For (almost) constant illumination and viewing angles – which holds true for the comparatively narrow overlapping areas between ADS takes – those physical or physically motivated models simplify to linear functions of the DN and can be approximated as such.

Regarding the spatial parameter variation, the RRN approach for ADS should at least account for across-take gradients to handle systematic BRDF effects as well as along-take tilting to model sun-angle changes and, to some degree, atmospheric variations. This is achieved through linear functions of image sample, x, and line, y. For linear histogram normalization as provided by equation (1), the correction reads:

$$DN_{RNN}\left(x,y\right)=\left(b_0+b_x x+b_y y\right)+\left(c_0+c_x x+c_y y\right)DN\left(x,y\right) \tag{2a}$$

The model can be generalized to polynomials for brightness and contrast:

$$DN_{RNN}\left(x,y\right)=P_b\left(x,y\right)+P_c\left(x,y\right)DN\left(x,y\right) \tag{2b}$$

Brightness and contrast parameters could be derived in an LSA, similar to the location-independent linear regression, which would result from a polynomial degree of 0.

Integrated Block Adjustment

Aiming for local radiometric adaptation within overlapping areas as well as global normalization of the mosaic, it suggests itself to combine these goals in an integrated least squares adjustment. Similar to Falala et al. (2008), the conditions for an overlap of images A and B follow from the identity of corrected data, based on equation (2):

$$0=\left[P_b^A\left(x^A,y^A\right)+P_c^A\left(x^A,y^A\right)DN^A\left(x^A,y^A\right)\right]-\left[P_b^B\left(x^B,y^B\right)+P_c^B\left(x^B,y^B\right)DN^B\left(x^B,y^B\right)\right] \tag{3}$$

These observation equations – with the polynomial coefficients as unknown parameters – have to be formulated for all radiometric tie points in all overlaps throughout the mosaic, independently for each image band. Such an adjustment would be under-determined as it lacks a radiometric reference. Furthermore, equation (3) has a very simple but undesired solution for the brightness and contrast polynomials: P_b = constant and P_c = 0; it has to be constrained, e.g. by preserving original radiometric properties, which leads to: P_b = 0 and P_c = 1. In case of a linear variation of parameters, i.e. for a polynomial degree of 1, it is possible to apply such conditions to the corner pixels and, therefore, to an entire image, which results in four equations per image and band for contrast and brightness:

$$0=P_b\left(x_{Corner},y_{Corner}\right) \tag{4a}$$

$$1=P_c\left(x_{Corner},y_{Corner}\right) \tag{4b}$$

The weighting between the observation equations (3) and the conditions (4) determines the balance between local normalization and preservation of original image statistics. Incorrect weighting can, on one hand, prevent normalization or, on the other hand, reduce the dynamic range. Practical test have shown that the adjustment is robust against a slightly wrong parameterization; accordingly, a default parameter can be used for most ADS blocks as long as the data are pre-corrected as described by Downey et al. (2010). The weight relation between the conditions (4a) and (4b) follows from the correction equation (2): Similar influence, and, therefore, similar effective changes of image brightness and contrast can be automatically achieved by utilizing the bands' average DNs as weight multipliers for contrast (4b) in comparison to brightness constraints (4a).

Global block homogenization is achieved by constraining the average DNs of each image and band towards a desired value, which can be the average of all input images or a subset of them, derived from reference images of neighboring blocks, or independent specifications. The correction equation itself is similar to (2), written at the image centers as the statistics themselves (average DNs of entire images) are location-independent:

$$\left\langle DN^{Mosaic} \right\rangle = P_b\left(x_{Center}, y_{Center}\right) + P_c\left(x_{Center}, y_{Center}\right)\left\langle DN \right\rangle \tag{5}$$

For an even better homogenization of the mosaic, additional equations of this type are formulated for minimum and maximum DNs, using a histogram count cutoff of 1.0% and 99.0%, respectively, to disregard outliers. Again, individual weighting, both in-between conditions and also in relation to the basic observation equations, can aim for either normalizing the mosaic or preserving the radiometry of original images. The latter is required for images of previously generated, neighboring mosaics that overlap with the block. Such reference images take part of the integrated block adjustment but remain unchanged by assigning very large weights for respective equations (4) and very low weights for equations (5). This weighting approach is preferred over omitting and/or modifying the equations above; part of the elegancy of such an integrated least squares adjustment lies in this flexibility. It is important to note that the individual treatment of different bands of multi-band imagery – those are in fact separate computations – does not cause color mismatches. Depending on the parameterization, the original color will be preserved or normalized to a (desired) average, both globally and locally.

The linear variation of contrast and brightness corrections results in 6, a location-independent parameterization in 2, and a quadratic polynomial in 12 RRN parameters per image and band. The implementation provides all three possibilities, i.e. polynomial degrees of 0, 1 and 2 with accordingly adapted constraints. However, tests show that the linear model is more robust than the quadratic one, especially across takes if points in overlaps can constrain only a smaller fraction along the image width.

Collection and Evaluation of Radiometric Tie Points

The RRN adjustment requires radiometric tie points: DN pairs for each band along with the location, x and y, in both overlapping images. As overlap areas of ADS images are usually vast and the information from all pixels is unnecessarily high to constrain a few parameters per image, allegedly corresponding points are sampled in a sparse pattern. The sample points undergo consistency checks, which comprise a relative DN difference and the across-band correlation as suggested by Scheidt et al. (2008), with a threshold of COR > 0.8:

$$COR = \frac{\sum_{NIR,R,G,B}\left(DN^{A} - \left\langle DN^{A}_{NRGB}\right\rangle\right)\left(DN^{B} - \left\langle DN^{B}_{NRGB}\right\rangle\right)}{\sqrt{\sum_{NIR,R,G,B}\left(DN^{A} - \left\langle DN^{A}_{NRGB}\right\rangle\right)^2}\sqrt{\sum_{NIR,R,G,B}\left(DN^{B} - \left\langle DN^{B}_{NRGB}\right\rangle\right)^2}} \tag{6}$$

Because our RRN aims for optimal adaptation of land, tie points in water areas are eliminated. Water is classified based on the NDVI < -0.1, computed from the NIR and red ADS bands:

$$NDVI = \frac{DN_{NIR} - DN_{R}}{DN_{NIR} + DN_{R}} \tag{7}$$

For the integrated adjustment, the number of radiometric tie points should be proportional to the area of the respective overlap, which inherently weights the influence on the overall image correction by the overlap's size. Therefore, remaining points are thinned in such a way that each overlap is divided into a grid and the desired num-

ber of points is randomly chosen within each grid cell to ensure an even distribution throughout the overlap. Water areas will result in empty cells and decrease the theoretical, size-dependent amount of points. This effect is desired; it omits water for the benefit of land normalization.

Because data I/O is the limiting factor for point collection performance and, therefore, the RRN adjustment in general, it is desired to use minified imagery (cp. Falala et al., 2008). The minification process modifies radiometry, which can be tolerated as long as the impact on the resulting parameters is negligible. This influence has been tested for a small ADS block of five neighboring images of similar lengths with pair-wise side overlaps of comparable sizes. Points have been sampled from the full resolution data (1:1) and from minification levels up to 512:1, evaluated as described, and thinned to an amount of 50 per overlap. Brightness and contrast corrections, b_0 and c_0, for all original and minified images are plotted in Figure 1. The test shows that RRN parameters up to level 8:1 nicely agree (within their standard deviations), which means that 1:1 imagery can be normalized using radiometric tie points from these minifications. Further minification introduces partly significant differences: It can be seen that contrast corrections tend to decrease while corresponding brightness corrections increase, which effectively causes a dynamic range reduction. The behavior is similar but not as pronounced when using a larger number of tie points (see also investigation below), so that in general a point sampling from 8:1 or even 16:1 minified imagery is suitable. That reduces the I/O to 1.6% or 0.4%, respectively, of the full resolution data – still being more time consuming than the actual adjustment computation, though.

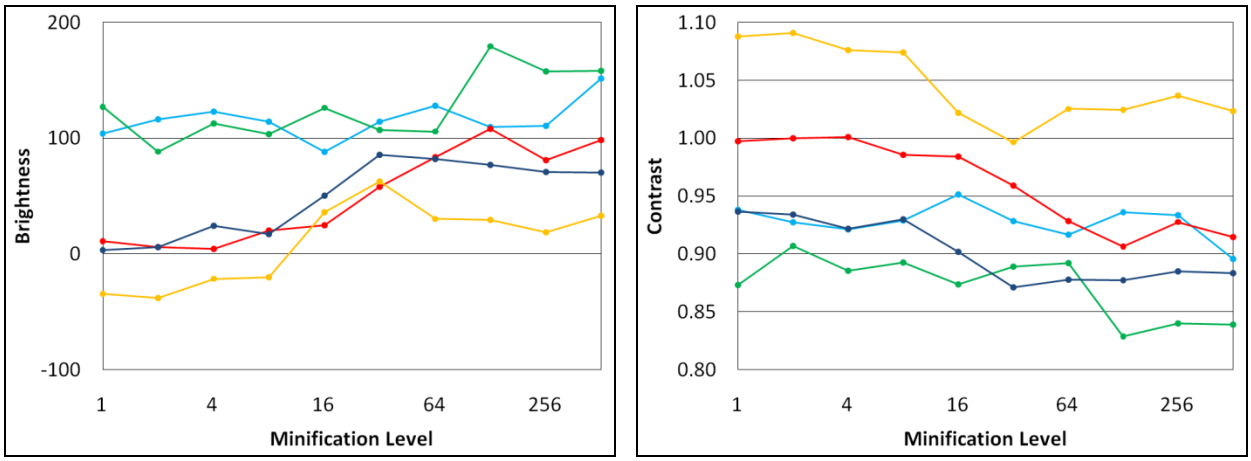

Figure 1. Brightness and contrast corrections for the red band of five images depending on the minification level (1:1 to 512:1) in which the radiometric tie points have been collected.

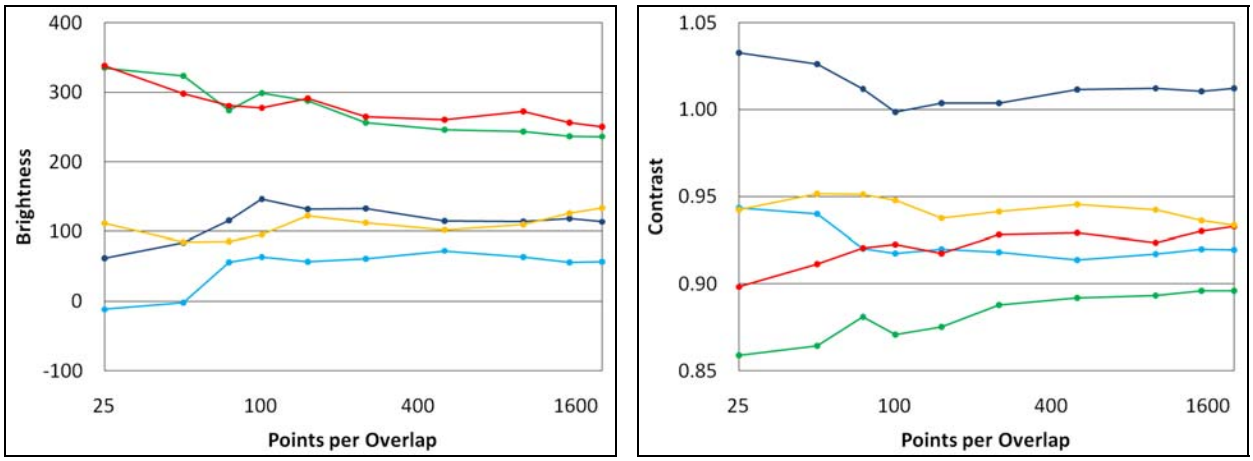

Figure 2. Brightness and contrast corrections for the NIR band of five images depending on the number of radiometric tie points.

For the same small test block, RRN parameters have been computed from different numbers of radiometric tie points, sampled from 1:1 data and leaving between 25 and 2000 points per overlap after evaluation and thinning. It turns out, while standard deviations generally decrease with an increasing amount of points, that the resulting parameters show only little dependency on the number of tie points when using at least 200; fewer points introduce uncertainty and should not be used (Figure 2). The image overlap of about 25% in this block translates to a minimum of 800 points per image area. The default value is set higher to 5,000 points, which is then internally scaled down to each individual overlap to ensure that the number of tie points used in computation is proportional to the overlap size.

Image Correction

The application of the resulting RRN parameters – location-dependent polynomial coefficients for brightness and contrast corrections – to each image band is straightforward and follows equation (2); reference images must not be modified. Except for preview purposes, the correction has to be applied to the full-resolution imagery, which should be carried out on a cluster of computing nodes to increase performance.

The corrected images form the input for subsequent mosaicking, i.e. for joining the individual images based on the determination of seam lines in the radiometrically adjusted overlaps and blending to ensure invisible transitions for remaining, minor radiometric differences. At North West Geomatics, the mosaicking process itself is carried out using third-party software.

RESULTS FROM PRODUCTION AND TESTING

Starting with the 2009 flying season, various ADS data sets have been processed with the presented RRN block adjustment at North West Geomatics, including USDA NAIP (National Agriculture Imagery Program) in the states of California, Montana and Washington, TNRIS (Texas Natural Resources Information System), and the Superior National Forest in Minnesota. Results for a typical ADS block in southern Texas are presented and discussed. This data has undergone initial radiometric corrections for camera calibration, atmospheric influences and BRDF differences – see end of this section for the application of the RRN approach to uncorrected ADS data.

Data Set

The area Texas South A has been flown by North West Geomatics in April 2009 for USDA NAIP in a GSD of 0.70 x 0.35 m. In altogether five flights with three different ADS cameras, a total of 36 takes has been captured. The data have been re-processed – including the RRN for mosaicking – and delivered to TNRIS as a 0.5 m FCIR product (TNRIS, 2010). The presented block covers an area from the Mexican border in the south and east to the Golf of Mexico, as far north as Baffin Bay; its largest extent is about 260 km x 190 km. Besides being imaged with different sensors and including one re-flight, the area contains a broad variety of features and also shows specular reflectance in water areas, which makes it a radiometrically challenging but, nonetheless, typical ADS block.

The initial atmospheric and BRDF corrections performed well in this area but there are remaining radiometric differences, most notable in the block overview in-between different flights and especially at the short re-flight in the north-central area. Apart from the essentially uncorrected bright water, across-take gradients are not visible in this block. Refer to Downey et al. (2010) for a comparison of original (calibrated) and corrected image data. The latter is shown here in Figure 3, top; it is the input for RRN.

Normalization and Results

The RRN has been computed fully automatically as described in the previous section, collecting radiometric tie points from 8:1 minified data and eliminating all points for which: 1) the DN difference exceeds 50% of the average DN in the respective overlap, 2) the across-band correlation is smaller than 0.8, and 3) the NDVI falls below -0.1; the latter classifies virtually all water and also some land features but leaves a sufficient amount of points for proper land normalization. The integrated adjustment has been based on altogether 21,974 points in 37 pair-wise overlaps. For linearly varying RRN parameters, a total of 216 unknowns had to be estimated per band (3 polynomial coefficients for each correction, contrast and brightness, for 36 images), which makes the adjustment highly redundant. All images have been treated equally, using default values for weights; no border conditions in terms of reference imagery have been introduced here.

Global image statistics as well as local overlap statistics, based on atmospheric and BRDF pre-correction and after RRN, are summarized in Tables 1 and 2, averaged (RMS) over all images of the block.

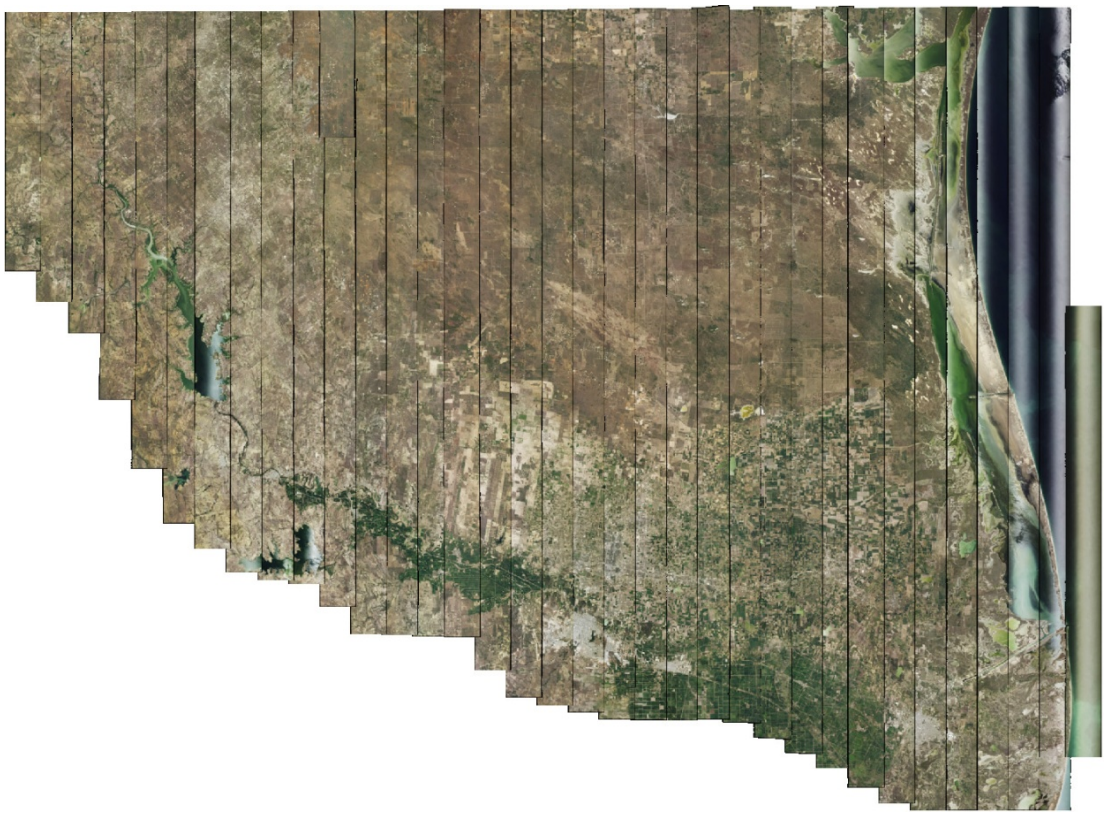

Figure 3. RGB overview of the block Texas South A before (top) and after RRN (bottom).

Table 1. Relative DN differences before and after RRN: average offset within overlaps and RMSE of all points.

Band	Atmospheric/BRDF		RRN	
	Avg. Diff.	RMSE	Avg. Diff.	RMSE
Red	5.6%	18.2%	1.4%	15.3%
Green	7.2%	18.0%	1.5%	14.2%
Blue	11.0%	18.5%	1.6%	11.1%
NIR	3.7%	17.2%	1.4%	14.6%

Table 2. Relative DN differences before and after RRN: minimum, maximum and average image DNs.

Band	Atmospheric/BRDF			RRN		
	Minima	Maxima	Averages	Minima	Maxima	Averages
Red	8.9%	20.5%	10.0%	6.2%	10.7%	0.3%
Green	9.2%	17.8%	9.5%	3.6%	9.3%	0.3%
Blue	9.0%	14.5%	9.1%	4.7%	9.1%	0.2%
NIR	13.0%	34.9%	12.1%	5.7%	12.5%	0.3%

Table 1 illustrates the significant improvement by RRN regarding the overall agreement in overlapping areas; the RMSE of individual points improves accordingly but not as much. This RMSE essentially reflects the radiometric variety within tie points; statistics could be further improved by applying more aggressive thresholds in the evaluation but it has been found that this tends to eliminate certain types of features, e.g. vegetation, which is not desired. The block homogenization is confirmed by Table 2: After RRN, average DNs match very closely, and the differences between minima and maxima reduce as well.

The global improvement is obvious when visually comparing the block before and after RRN adjustment (Figure 3). Transitions between individual lifts and especially at the re-flight improve significantly. As expected from the approach, water areas are not adapted; they change slightly according to the RRN corrections derived for land, which are applied to all image content. The generally desired homogenization, however, modifies especially the color of the eastern-most image, which is virtually all (originally blue) water, towards the green of the land surface. Although it is not critical in this case, the effect could be avoided by assigning individual adjustment weights for that image to better maintain the original color.

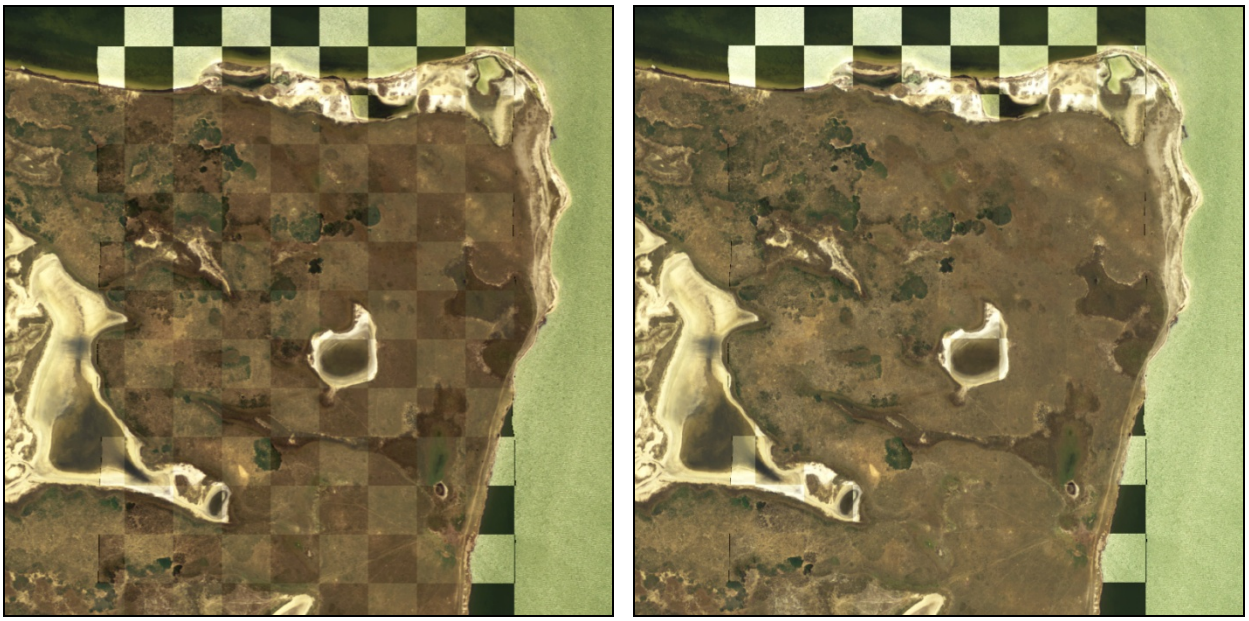

Figure 4. RGB checkerboard representation of an overlap at Baffin Bay before (left) and after RRN (right).

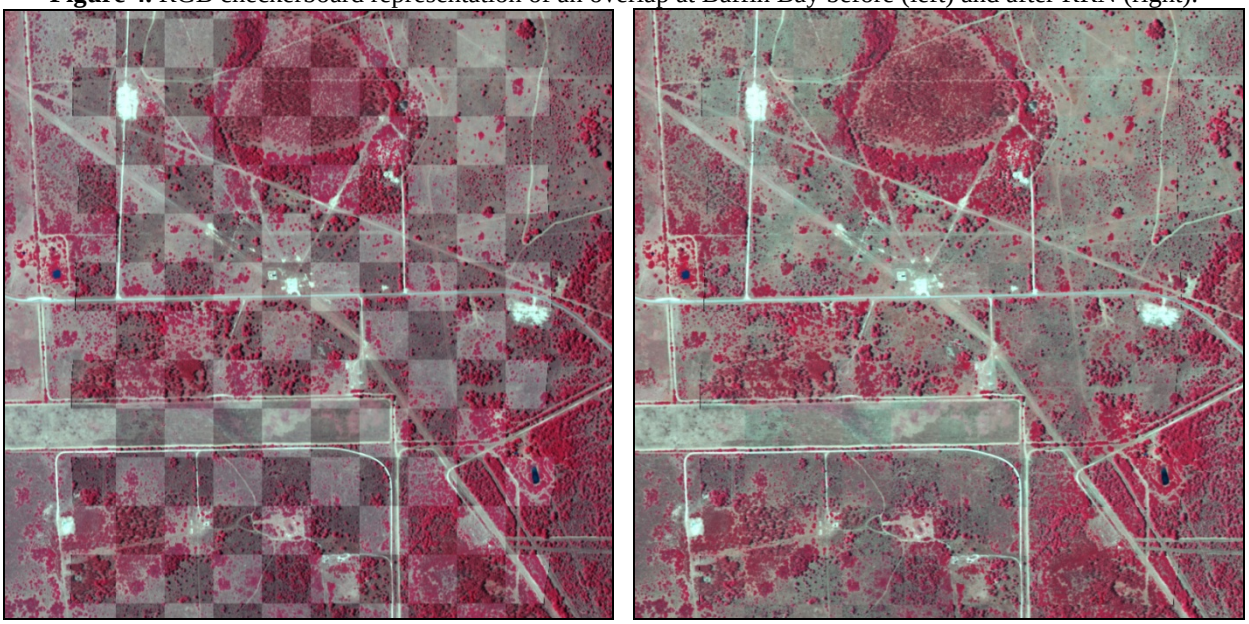

Figure 5. FCIR checkerboard representation of an overlap in the northern part of the block before (left) and after RRN (right).

Local normalization is best illustrated by applying a checkerboard pattern within the reviewed image overlaps. On the peninsula in Baffin Bay (Figure 4), e.g., the improvement by RRN is clearly recognizable; the checkerboard virtually disappears on land but not in water, where the initially large radiometric differences – caused by specular reflectance in the eastern flight-line – are even slightly exaggerated. Apart from the correct normalization result in the land area, this overlap suggests that it would not be feasible to adapt both land and water by using a single RRN model. Figure 5 gives a similarly successful example for the normalization over a land area in false-color infrared (FCIR).

While these two cases feature a similar difference in brightness and contrast throughout all bands, the pre-corrected re-flight image appears bluish, suggesting that the initial radiometric correction did not remove all atmospheric haze (Figure 6, left). With RRN, the color differences have been adapted and agree with the rest of the corrected block (see also Figure 3); however, the checkerboard pattern can still be identified, especially in trees, which can be explained by different illumination and, accordingly, also different shadows. Nevertheless, the result should allow for placing a seam-line within that overlap and eventually achieve a uniform mosaic with a smooth transition after blending.

Normalization without Prior Atmospheric and BRDF Corrections

To illustrate the potential of the presented RRN approach, the Texas South A block has been adjusted based on only calibration-corrected imagery. The re-flight overlap before and after this correction is set in contrast in Figure 7. The input imagery clearly shows major brightness differences, which are explained by significantly different illumination conditions: The re-flight data had been captured under very low light, starting 5:14 p.m. local time, while the neighboring flight-line started at 11:04 a.m., i.e. at a high sun angle. The predominantly blue color is caused by the atmospheric haze, which results from flight altitudes of about 6.5 km above ground. This data set demonstrates the necessity of initial atmospheric and BRDF corrections for any serious production work – see Downey et al. (2010) for overviews of the entire block with and without these corrections applied.

The RRN test has been run with the default parameterization, which includes global mosaic homogenization based on the average brightness and, accordingly, color; this explains the blue tone in the normalized data. Apart from the undesired color and limited contrast, the overlapping area is in similarly good agreement as with prior atmospheric and BRDF corrections (cp. Figures 6 and 7). Slight across-take gradients are introduced by RRN in some other images of the calibrated-only block, which is not shown here. (It should be remarked that the occurrence of such gradients might have been prevented or reduced by a better parameterization in terms adapted weights.

However, the main focus of this test was general feasibility and not the optimal normalization of essentially invalid data.)

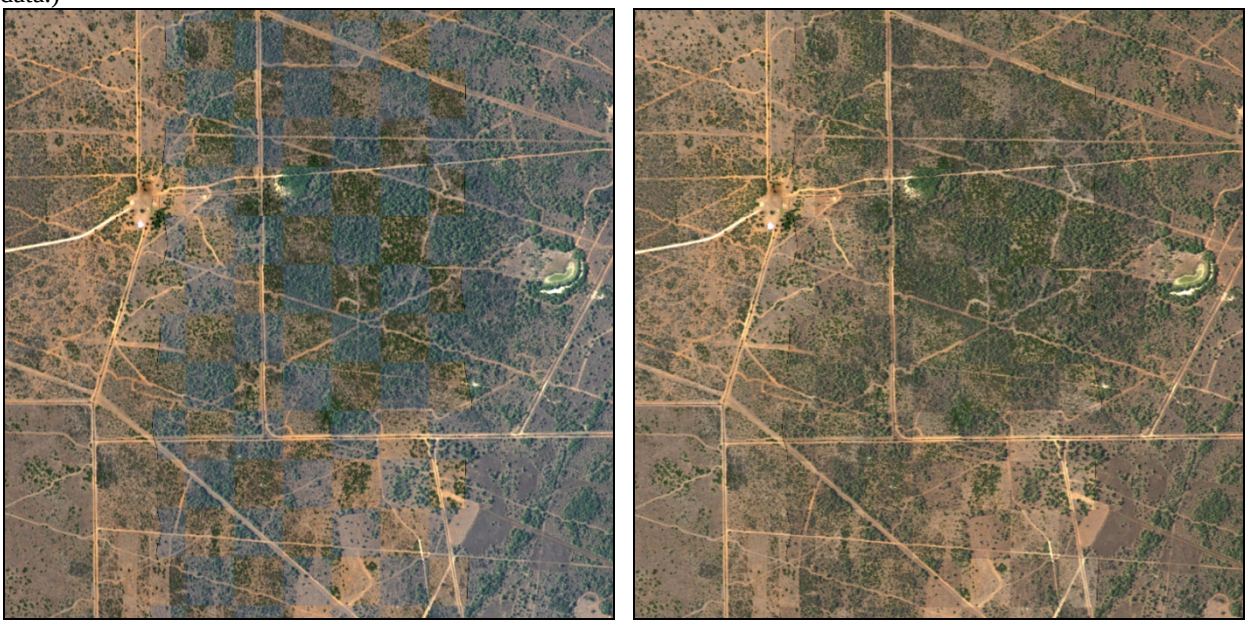

Figure 6. RGB checkerboard representation of the overlap between the re-flight (right part) and its neighboring image before (left) and after RRN (right).

Figure 7. RGB checkerboard representation of the overlap between the re-flight (right part) and its neighboring image before (left) and after RRN (right), based on calibrated input data.

CONCLUSION

An RRN approach for large blocks of line-scanner imagery has been presented, which allows for local adaptation of overlapping areas as well as for global homogenization. Based on pre-corrected data, it has been shown that a fully automatic RRN can adjust the vast majority of DN differences and provide a radiometrically uniform data set for

mosaicking. Although the adjustment of uncorrected input data is not a valid use-case, substantial radiometric variation throughout a large ADS block might be; it has been demonstrated that such a block can be processed if needed.

Within North West Geomatic's production, the normalization approach has been successfully applied to various data sets and considerably improved orthoimage mosaicking. Therefore, the calibration, atmospheric and BRDF corrections as described by Downey et al. (2010) in combination with this RRN research effort provide the entire radiometric processing chain for Leica ADS imagery.

REFERENCES

Afek, Y., and A. Brand, 1998. Mosaicking of Orthorectified Aerial Images, *Photogrammetric Engineering & Remote Sensing, 64(2)*:115-125.

Brown, M., and D.G. Lowe, 2007. Automatic Panoramic Image Stitching Using Invariant Features, *International Journal of Computer Vision, 74(1)*:59-73.

Canty, M.J., A.A. Nielsen, and M. Schmidt, 2004. Automatic Radiometric Normalization of Multispectral Imagery, *Remote Sensing of Environment, 91(3,4)*:441-451.

Ding, L.-X., B. Zhou, and R.-C. Wang, 2005. Comparison of Five Radiometric Normalization Techniques for Remote Sensing Monitoring, *Journal of Zhejiang University, 31(3)*:269-276.

Downey, M., R. Uebbing, S. Gehrke, and U. Beisl, 2010. Radiometric Processing of ADS Imagery: Using Atmospheric and BRDF Corrections in Production, *ASPRS Annual Conference, San Diego, CA* (this issue).

El Hajj, M., A. Begue, B. Lafrance, O. Hagolle, G. Dedieu, and M. Rumeau, 2008. Relative Radiometric Normalization and Atmospheric Correction of a SPOT 5 Time Series, *Sensors, 8*:2774-2791.

Falala, L, R. Gachet, and L. Chunin, 2008. Radiometric Block-Adjustment of Satellite Images - Reference3D Production Line Improvement, *Int. Arch. Phot. & Rem. Sens., Beijing, China, 37(B4)*:319-324.

Galiatsatos, N., D.N.M. Donoghue, D. Knox, and K. Smith, 2007. Radiometric Normalization of Multisensor/Multitemporal Satellite Images with Quality Control for Forest Change Detection, *International Workshop on the Analysis of Multi-temporal Remote Sensing Images, Leuven, Belgium*.

Homer, C.G., R.D. Ramsey, T.C. Edwards Jr., and A. Falconer, 1997. Landscape Cover-Type Modeling Using a Multi-Scene Thematic Mapper Mosaic, *Photogrammetric Engineering & Remote Sensing, 63(1)*:59-67.

Hong, G., 2007. Image Fusion, Image Registration, and Radiometric Normalization for High Resolution Image Processing, *University of New Brunswick, Technical Report No. 247*.

Jantzen, D.T., A.L. Fredeen, and R.D. Wheate, 2006. Radiometric Correction Techniques and Accuracy Assessment for Landsat TM Data in Remote Forested Regions, *Canadian Journal of Remote Sensing, 32(5)*:330-340.

Jessop, R.K., and W. Schickler, 2000. Optimal Balancing and Enhancement of Color and Contrast fro Ortho Photo Mosaicking, *ASPRS Annual Meeting, Washington, D.C.*

Nielsen, M.O., 2004. True Orthophoto Generation, *Master Thesis, Technical University of Denmark, Lyngby*.

Nobrega, R.A.A., and J.A. Quintanilha, 2004. Comparative Analysis of Automatic Digital Image Balancing and Standard Histogram Enhancement Techniques in Remote Sensing Imagery, *Revista Brasilera de Cartografia, 56(1)*: 55-64.

Over, M., B. Schöttker, M. Braun, and G. Menz, 2003. Relative Radiometric Normalization of Multitemporal Landsat Data - A Comparison of Different Approaches, *Proceedings IGARSS, Toulouse, France*.

Scheidt, S., M. Ramsey, and N. Lancaster, 2008. Radiometric Normalization and Image Generation of ASTER Thermal Infrared Data: An Application to Extensive Sand Sheets and Dune Fields, *Remote Sensing of Environment, 112*:920-933.

TNRIS, 2010. 2008-2009 Texas Orthoimagery Program 0.5-meter DOQQs Now Available, *Texas Natural Resources Information System, www.tnris.state.tx.us/news.aspx?id=1384* (accessed March 1, 2010).

Tsai, V.J.-D., and Y.-T. Huang, 2005. Automated Image Mosaicking, *Journal of the Chinese Institute of Engineers, 28(2)*:329-340.

Uyttendaele, M., A. Eden, and R. Szeliski, 2001. Eliminating Ghosting and Exposure Artifacts in Image Mosaics, *Proceedings IEEE Conference on Computer Vision and Pattern Recognition, 2*:509-516.

Xandri, R., F. Perez-Aragües, V. Pala, and R. Arbiol, 2005. Automatic Generation of Seamless Mosaics over Extensive Areas from High Resolution Imagery, *Proceedings International Cartographic Conference*.

Yuan, D., and C.D. Elvidge, 1996. Comparison of Relative Radiometric Normalization Techniques, *ISPRS Journal of Photogrammetry and Remote Sensing, 51(3)*:117-126.

Yang, X., and C.P. Lo, 2000. Relative Radiometric Normalization Performance for Change Detection from Multi-Date Satellite Images, *Photogrammetric Engineering & Remote Sensing, 66(8)*:967-980.